

REGIONAL EVENT IDENTIFICATION RESEARCH IN EASTERN ASIA

Steven R. Taylor, Xiaoning (David) Yang, W. Scott Phillips, Howard J. Patton, Monica Maceira, Hans E. Hartse,
and George E. Randall

Los Alamos National Laboratory

Sponsored by National Nuclear Security Administration
Office of Nonproliferation Research and Engineering
Office of Defense Nuclear Nonproliferation

Contract No. W-7405-ENG-36

ABSTRACT

We describe ongoing studies of broad-area regional-event identification in Eastern Asia. The goal of our work is to provide a framework that allows for accurate identification, operational transparency and clear reporting to non-technical decision makers. The underlying methodologies need to have a clear physical basis packaged in a sound statistical framework having proper uncertainty estimates.

The Magnitude and Distance Amplitude Correction (MDAC) methodology is used to correct regional seismic amplitudes for propagation effects and earthquake source scaling. We correct amplitudes rather than predefining various phase ratios because all information is retained from which to construct discriminants. Because signals from explosions are highly dependent on near-source material properties and emplacement conditions, it is difficult to *a priori* select discriminants from un-calibrated regions. The MDAC approach adds much flexibility to the problem and allows for construction of numerous combinations of discriminants in a multivariate setting using Gaussian statistics. The MDAC parameters are specified using an earthquake source model that allows for non-constant stress drop and variable P and S wave corner frequency scaling. Because the earthquake model is inappropriate for explosions it is assumed that a poor fit will be obtained for explosions and allow for their identification. MDAC calibration parameters for a region are updated when corresponding geophysical information is available. Seismic moments and earthquake source scaling are computed from coda M_w values and attenuation corrections are from regional phase tomography. The MDAC parameters can be used rapidly in an operational setting.

We are also developing regional surface wave discriminants (e.g. $m_b - M_s$). These studies involve validation of existing surface slowness tomographic models and refining where appropriate (Yang *et al.*, 2002). Tomographic models at shorter periods are being developed and refined in selected regions. These studies lower detection thresholds and allow for discrimination at lower magnitudes. Surface-wave attenuation maps are also being developed using a Bayesian approach. *A priori* tomographic models are constructed using two-station amplitude-ratio measurements. Single-station measurements are then inverted for higher resolution maps. In order to isolate and enhance the surface-wave signal, we apply a phase-matched filter constructed from surface-wave group-velocity maps before making the spectral-amplitude measurement. The filtering eliminates, or greatly reduces the ambiguity due to multi-pathing and improves the fidelity of our measurements. We also use the theoretical source spectra to guide the measurement and gauge the quality of the data. We found general correlation between the two-station attenuation map and geological provinces of the region. Preliminary results also indicate that attenuation models are not highly dependent on the source of event parameters (CMT or recent regional studies) that we use to correct the amplitudes.

OBJECTIVE

The objective of this work is to provide methodologies and calibration for robust event identification at reduced monitoring magnitude thresholds.

RESEARCH ACCOMPLISHED

Magnitude and Amplitude Distance Corrections (MDAC)

A fundamental problem associated with event identification lies in deriving corrections that remove path and earthquake source effects on regional phase amplitudes used to construct discriminants. Our goal is to derive a set of physically based corrections that are independent of magnitude and distance, and amenable to multivariate discrimination by extending the technique described in Taylor and Hartse (1998) and Taylor *et al.* (2002). The MDAC procedure for correcting regional seismic amplitudes for seismic event identification has been modified to include more realistic earthquake source models and source scaling (MDAC2; Walter and Taylor, 2002).

To model and understand regional seismic spectra, we need to break down the observations into their component parts. The observed instrument-corrected regional phase spectra can be thought of as a convolution between the source and the path. In the frequency domain we can write this out as a cascading multiplication:

$$A_o(\omega, R) = S(\omega)G(R)P(\omega)B(\omega, R), \quad (1)$$

where ω is the angular frequency; R is the distance and:

- $S(\omega)$ is the source spectrum;
- $G(R)$ is the geometrical spreading;
- $P(\omega)$ is the frequency dependent site effect;
- $B(\omega, R)$ is the apparent attenuation.

Here we have split the path effect into three pieces: 1) a frequency-independent geometrical-spreading component, 2) a distance-independent and frequency-dependent site-effect component, and 3) an apparent attenuation component.

The MDAC2 prediction of the observed, instrument-corrected spectra is then given by the same equation except now we estimate each of the components:

$$A_m(\omega, R) = S(\omega)G(R)P(\omega)B(\omega, R). \quad (2)$$

We linearize equation (2) by taking the logarithm of both sides:

$$\log A_m(\omega, R) = \log S(\omega) + \log G(R) + \log P(\omega) + \log B(\omega, R). \quad (3)$$

To remove the data trends with distance and magnitude, we correct the observed spectrum, $A_o(\omega, R)$, by subtracting the log of the MDAC2 spectrum in equation (3):

$$\log A_c(\omega, R) = \log A_o(\omega, R) - \log A_m(\omega, R). \quad (4)$$

These corrected spectra or residuals can then be kriged to further reduce un-modeled path effects (e.g. Schultz *et al.*, 1998).

For a given station and source region, a number of well-recorded earthquakes are used to estimate source and path corrections. In the MDAC2 formulation, we generalize the Brune (1970) earthquake source model with a more physical apparent-stress model that can represent non-constant stress-drop scaling. We also include a parameter that allows for variable P-wave and S-wave corner frequency scaling. The discrimination power in using corrected

amplitudes lies in the assumption that the earthquake model will provide a poor fit to the signals from an explosion. The propagation model consists of a frequency-independent geometrical spreading and frequency-dependent power-law Q . We incorporate regional phase attenuation tomographic models to replace a constant Q_0 model (Phillips *et al.*, 2000; Taylor *et al.*, 2003).

A grid search is performed simultaneously at each station for all recorded regional phases over stress-drop, geometrical spreading, and frequency-dependent Q to find a suite of good-fitting models that remove the dependence on M_w and distance. Very stable moment magnitude measures from regional coda wave envelopes that have been tied to independently derived regional seismic moments are incorporated. We also solve for frequency-dependent site/phase excitation terms. Once a set of corrections is derived, effects of source scaling and distance as a function of frequency are applied to amplitudes from new events prior to forming discrimination ratios. Thus, all the corrections are tied to M_w and distance and can be applied very rapidly in an operational setting. Moreover, phase-amplitude residuals as a function of frequency can be spatially interpolated (e.g., using kriging) and used to construct a correction surface for each phase and frequency. The spatial corrections from the correction surfaces can then be applied to the corrected amplitudes based only on the event location. The correction parameters and correction surfaces can be developed offline and entered into an online database for pipeline processing providing multivariate-normal corrected amplitudes for event identification (Figure 1).

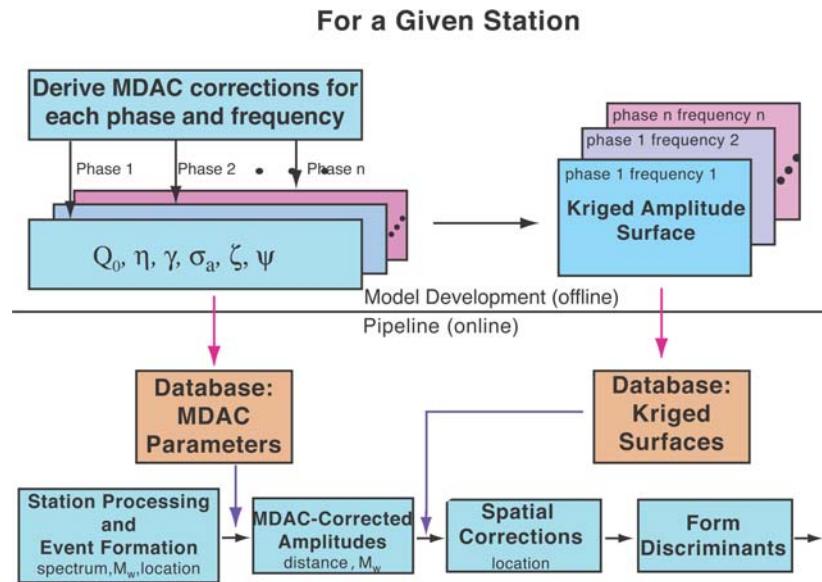


Figure 1. Example flowchart illustrating how the MDAC method can be combined with spatial interpolation (e.g., kriging) to develop database parameters to provide amplitude corrections for regional event identification in near-real time. These parameters can easily be incorporated into an operational pipeline to correct amplitudes from a new event for identification purposes.

As an illustration of the MDAC methodology, we present results from the IRIS (Incorporated Research Institutes for Seismology) GSN (Global Seismic Network) station MAKZ (Makanchi, Kazakhstan). The data are from four Lop Nor nuclear explosions and 412 earthquakes located in a region around Lop Nor extending between 35° and 50° N latitude and 80° and 100° E longitude. We corrected all amplitudes that passed the signal-to-noise cutoff of 1 using pre-phase noise including the four Lop Nor nuclear explosions. Figure 2 shows the corrected log amplitudes for each phase as a function of frequency for all four phases. We have also identified four earthquakes occurring within 50 km of the Lop Nor test site. As is expected, the corrected amplitudes for the earthquakes are very close to zero mean, and χ^2 goodness-of-fit tests show most frequency bands are normally distributed. The explosions show a significantly different pattern than the earthquakes. This is not unexpected, since we are using an earthquake model to fit the data. The misfit is particularly severe for Pn as can be seen by the high residuals at intermediate and high frequencies. As will be further illustrated below, the plot in Figure 2 is interesting in that it can be used as a guide in selecting individual discriminants that provide good separation between earthquakes and explosions. For example, it can be seen that a high frequency Pn to low-frequency Sn or Lg cross-spectral ratio will give excellent separation

between the earthquakes and explosions (as noted by Hartse *et al.*, 1997). Additionally, a Pn, Pg, or possibly even an Sn spectral ratio will provide good separation. These observations reinforce our earlier comments about the potential restrictions on discrimination performance by *a priori* selecting ratios.

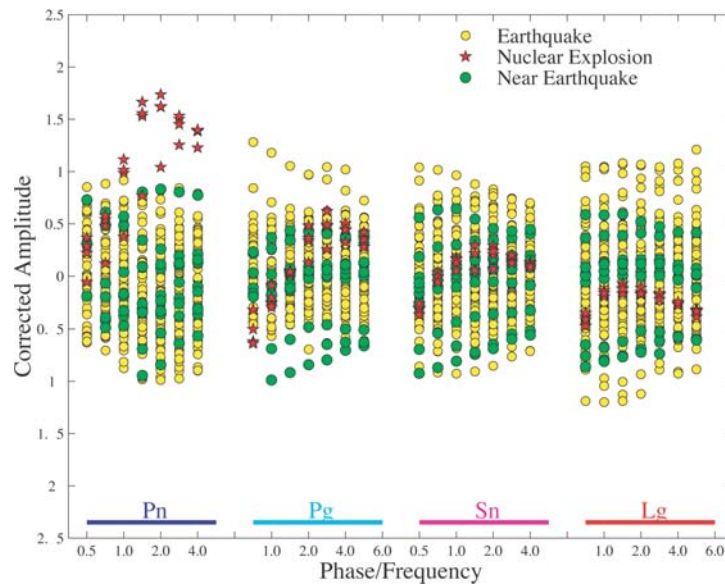


Figure 2. MDAC-corrections in log amplitudes for each phase as a function of frequency at MAK/MAKZ including the 4 Lop Nor nuclear explosions. Four earthquakes within 50 km of Lop Nor are also identified. Each amplitude is normalized by the lowest-frequency Lg amplitude (0.5-1 Hz).

At this point we can directly make traditional discrimination plots from the corrected amplitudes shown in Figure 2 by simply taking differences (log ratios) using any combination of phases and frequencies. Examples of four discriminants were discussed in Taylor, *et al.* (2002). The separation between the earthquakes and explosions is quite good (including the Lop Nor earthquakes). Note that in all cases the discrimination performance is excellent and trends are removed with magnitude. The separation between the Lop Nor explosions and earthquakes is very good indicating that the discriminants are based on source or very near-source differences between the two different source types. Thus, utility of the MDAC procedure allows us to retain all amplitude information as a function of phase and frequency.

Short-Period Rayleigh-Wave Group-Velocity Tomography

Short-period, high-resolution surface-wave slowness tomographic maps are necessary to lower detection thresholds and allow for discrimination at lower magnitudes. We focus on the region between 70° and 95° E longitude and 35° and 50° N latitude. We used the PDE catalog to guide the collection of earthquake data from IRIS DMC. We retrieved broadband waveform data from more than 1,100 events that occurred in the area between January 1997 and May 2002. Waveforms were obtained from four different networks (IRIS/USGS, IRIS/IDA, CDSN, and Geoscope) comprising 13 individual stations. Using multiple-filter analysis (Dziewonski *et al.*, 1969; Herrmann, 1973) and phase-matched filter (Herrin and Goforth, 1977) techniques, we measured the dispersion characteristics of the signals between 5 and 30 seconds. These Rayleigh-wave group velocity dispersion curves were used to compute high-resolution (0.5° cell) slowness tomographic maps for each period.

We have adopted a Bayesian tomography method (Tarantola, 1987; Taylor *et al.*, 2003) to solve the equation that relates the travel-time data with the velocity structure

$$\mathbf{d} = \mathbf{G}\mathbf{m}, \quad (5)$$

where \mathbf{G} represents the matrix containing path-length elements; \mathbf{m} is the vector of unknown block slowness, and \mathbf{d} is the data vector. The Bayesian solution of equation (5) is

$$\mathbf{m} = \mathbf{m}_0 + (\mathbf{G}^T \mathbf{C}_d^{-1} \mathbf{G} + \mathbf{C}_{m_0}^{-1})^{-1} \mathbf{G}^T \mathbf{C}_d^{-1} (\mathbf{d} - \mathbf{G}\mathbf{m}_0), \quad (6)$$

where \mathbf{m}_0 is the *a priori* model, and \mathbf{C}_d and \mathbf{C}_{m_0} are the data and *a priori* model covariance matrices respectively. Within the Bayesian framework, statistical characteristics of the data and the *a priori* information are utilized in the inversion to constrain the results and their uncertainty.

We used a declustering technique to remove the effect of event clusters. Instead of taking the average of the measurements in a cluster, we retain all the measurements, but down-weight each measurement with a weighting factor that is inversely proportional to the number of events that fall within the same cluster (Isaaks and Srivastava, 1989). The weighting factor is incorporated in the data covariance matrix \mathbf{C}_d . Global and regional 1° group-velocity maps are available from previous studies (Levshin *et al.*, 2001; Ritzwoller and Levshin, 1998; Stevens *et al.*, 2001). These maps were evaluated (Yang *et al.*, 2002) and proved to be effective to construct an *a priori* model for the region of interest.

The slowness tomographic map for 10s is shown in Figure 3 as an example. The inverted model is similar, to some extent, to the *a priori* model, but it shows more structure and it is of higher resolution (0.5° cell compared to 1° cell for the *a priori* model). The tomographic patterns correlate really well with known geologic and tectonic features in the area. Accumulations of relatively young sediments across Eurasia are greater than on any other continent due to the continuing rapid uplift across central Asia because of the collision between the Eurasian plate and the Indian plate. The tomography maps display low velocities associated with the known sedimentary basins – Tarim, Junggar and Qaidam basins - in the area of central Asia under study. On the other hand, high velocities appear associated with mountainous tectonic features such as the Tien Shan Mountains. These improved high-resolution, short-period tomography maps can be used to lower the M_b detection thresholds to be used for construction of regional $m_b - M_s$ discriminants.

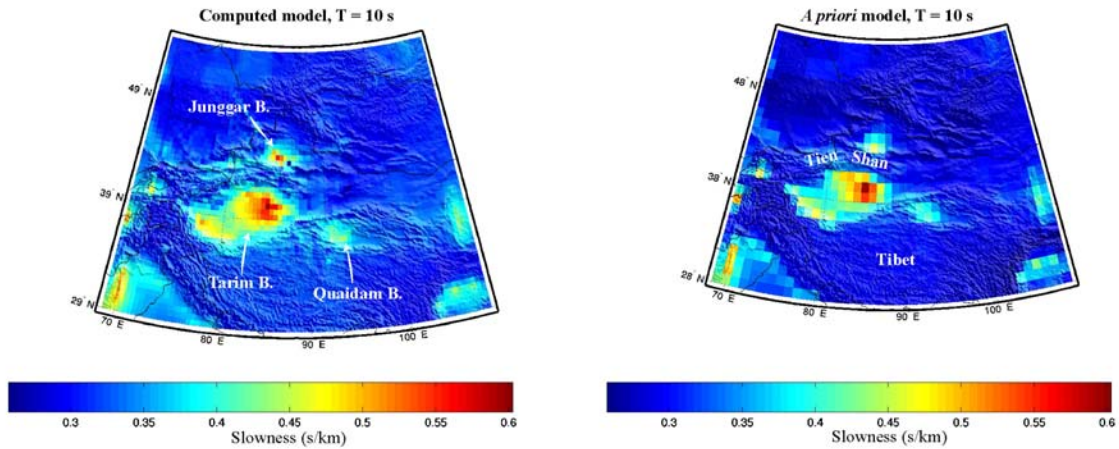


Figure 3. A comparison between the inverted Rayleigh-wave slowness tomographic map at 10 second and the *a priori* model. Warm colors represent low group velocities and cool colors indicate high velocities.

20-sec Rayleigh-Wave Attenuation Tomography

The $m_b - M_s$ relationship has proven to be an effective teleseismic discriminant. In order to extend its applicability to regional distances, lateral heterogeneity in the crust and upper mantle needs to be accounted for. We are mapping out another aspect of these heterogeneities by developing 20-sec Rayleigh-wave attenuation models for central Asia ($15^\circ - 65^\circ$ N; $70^\circ - 130^\circ$ E). We take two steps in developing the attenuation model. First, we use two-station amplitude-ratio measurements, which are less affected by source-parameter error than single-station amplitude measurements, to obtain a coarse-grid (5° cell) model with a tomographic inversion. We then invert for the final model (2° cell) with single-station measurements, which have much better path coverage. We have adopted the

Bayesian approach discussed in last section for the tomography as well (equation (6)). The coarse-grid model is used as the *a priori* model in the final inversion.

The attenuation term $B(\omega, R)$ in equation (1) for surface waves can be expressed as $B(\omega, R) = \exp(-\lambda(\omega)R)$, where λ is the attenuation coefficient. An equivalent of equation (3) for surface waves, after geometrical-spreading correction, then becomes

$$\ln A(\omega, R) = \ln S(\omega) + \ln P(\omega) - \lambda(\omega)R. \quad (7)$$

If two seismic stations lie on the same great-circle path that goes through an earthquake source, the geometrical-spreading corrected amplitude ratio between the two stations is

$$\frac{A(\omega, R_1)}{A(\omega, R_2)} = \frac{P_1(\omega)}{P_2(\omega)} e^{-\lambda(\omega)(R_2 - R_1)},$$

or in the logarithm domain as

$$\ln \frac{A(\omega, R_1)}{A(\omega, R_2)} = \ln P_1(\omega) - \ln P_2(\omega) - \lambda(\omega)(R_2 - R_1), \quad (8)$$

where λ is the average attenuation coefficient of the medium between the two stations. In the tomographic inversion, we discretize the last term in equations (7) and (8) and group multiple observations together. In a matrix form, the problem is expressed as equation (5). Using 20-sec Rayleigh-wave spectral amplitudes, we solve for the model \mathbf{m} , which contains discretized attenuation coefficients, site-effect and source-effect terms, with equation (6).

Surface-wave generation and propagation are affected by many factors such as source mechanism and location, path heterogeneity and site response (e.g., Mitchell, 1995). In order to reduce the error in the amplitude measurements caused by these factors or their uncertainties, especially the path heterogeneity, we designed a measuring tool that makes use of phase-matched filters and other source and path information available to achieve reliable measurements. We use Rayleigh-wave group-velocity models developed by Levshin *et al.* (2002), Ritzwoller and Levshin (1998) and Stevens *et al.* (2001) to construct phase-matched filters. We then calculate the cross-correlation between the instrument-corrected data and the phase-matched filter for the same path and window the cross-correlation around the peak associated with the main arrival. In many cases, this technique effectively isolates the direct arrival from multi-pathing, thus reduces the error introduced by off-great-circle propagation and focusing. Using source parameters from the Harvard CMT catalog, we also plot source radiation patterns and theoretical source spectra along with great-circle paths and data spectra to help guide our measurement and gauge the quality of the data. Figure 4 gives an example of the effectiveness of the phase-matched filters in extracting clean amplitude spectra.

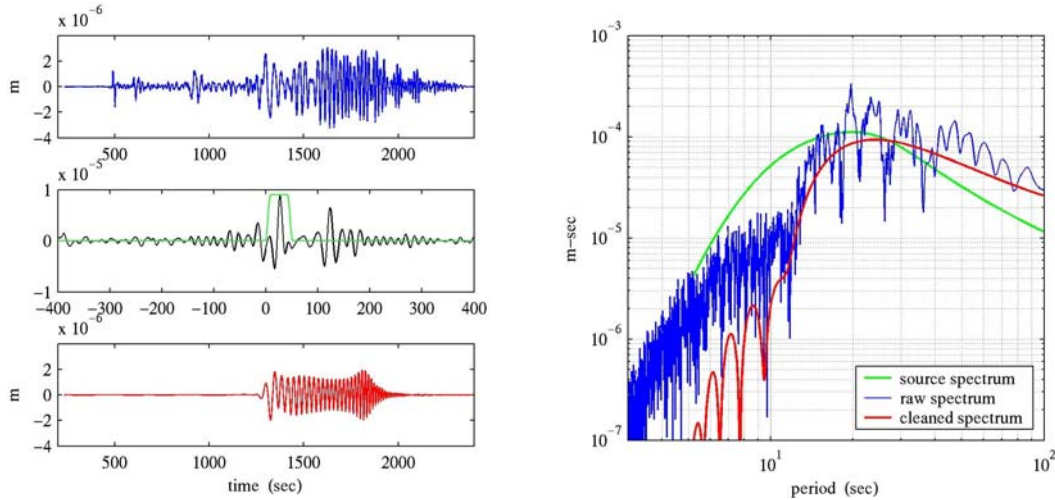


Figure 4. An example showing the phase-match filtering technique. The data are from an event in south RyuKyu Islands southeast of China and recorded at station Hyderabad in India. On the left, the top plot shows the original seismogram. Cross-correlation between the seismogram and the phase-matched filter for this path is plotted in the middle along with a window isolating the direct arrival. The cross-correlation clearly shows a second arrival indicating multi-pathing. The lower plot on the left is the cleaned seismogram. The plot on the right shows the theoretical source spectrum, the raw-data spectrum and the cleaned data spectrum. The cleaned spectrum is smooth and has a similar shape as the theoretical spectrum. The gentler roll-off of the theoretical spectrum toward lower periods is probably due to the fact that no attenuation was included in its calculation.

With the criterion that the azimuth difference between the two stations in a station pair is less than or equal to 2° , we have made 890 two-station amplitude-ratio measurements for 206 inter-station paths. Figure 5a shows the path coverage of the measurements and Figure 5b plots the geometrical-spreading corrected amplitude ratio as a function of inter-station distance.

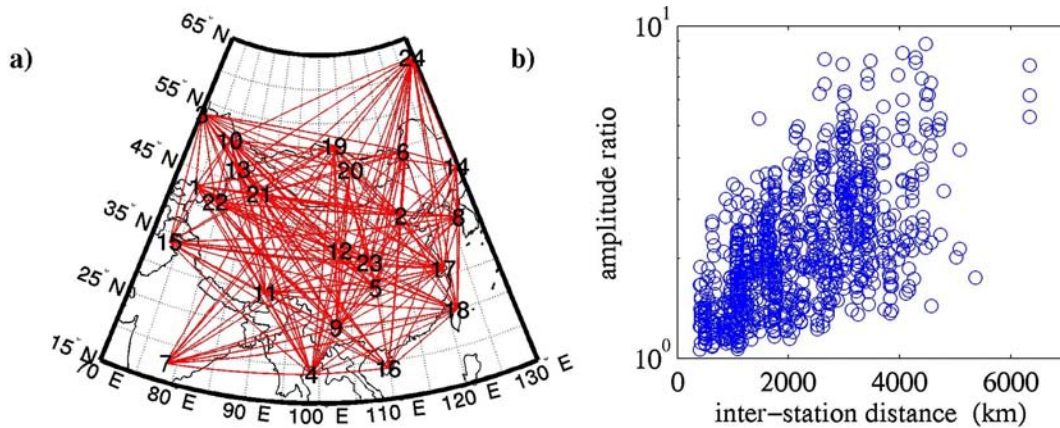


Figure 5. a) Path coverage of the two-station amplitude-ratio measurements. Station locations are marked by numbers. Grid lines define the discretization of the region for the first-step, coarse-grid inversion. b) Amplitude ratio as a function of inter-station distance. The logarithms of the ratios exhibit a linear trend as is expected.

For the two-station amplitude-ratio inversion, we assumed that the data are independent of each other. We then used a quality factor that we assigned to the data when we made the measurements to construct the diagonal elements of the data variance matrix C_d . Because we usually have multiple measurements for each inter-station path, we down-weighted each measurement according to the number of measurements for that path by a weighting factor

incorporated in C_d . We also used a diagonal matrix for the *a priori* model covariance and conducted a grid search to select reasonable values for the *a priori* model and its variance based on the behavior of data residuals. Figure 6 displays the inverted attenuation coefficient model and site-effect terms for 20-sec Rayleigh waves. The estimated attenuation coefficients span a range that corresponds to Q values from about 120 to about 785. Some of the broad correlation between the attenuation model and the geological and tectonic provinces of the region include high attenuation in western China, Tibetan Plateau, Sichuan Basin, Bay of Bengal, east China seas and Baikal Rift, and low attenuation in India and North China Platform. Due to the relatively sparse path coverage, there could be spurious features in the model. We believe that the single-station inversion will reduce the error in this *a priori* model and produce more accurate results.

CONCLUSIONS AND RECOMMENDATIONS

Event identification studies in eastern Asia involve development of algorithms for constructing discriminants as well as applying the algorithms for station calibration. Our research outlined in this paper has focused on regional seismic discrimination using MDAC corrected amplitudes and regional $m_b - M_s$ discriminants.

Our ongoing work in the surface-wave attenuation tomography is to make single-station spectral amplitude measurements and prepare for the final model inversion. Preliminary trial inversions with single-station amplitude data indicates that correcting the amplitudes with source parameters from different catalogs (CMT and recent regional studies) has minor effects on the resulting attenuation model (< 10%). We are also investigating the issue of constructing more realistic data and model covariance matrices with non-zero off-diagonal elements based on covariance models.

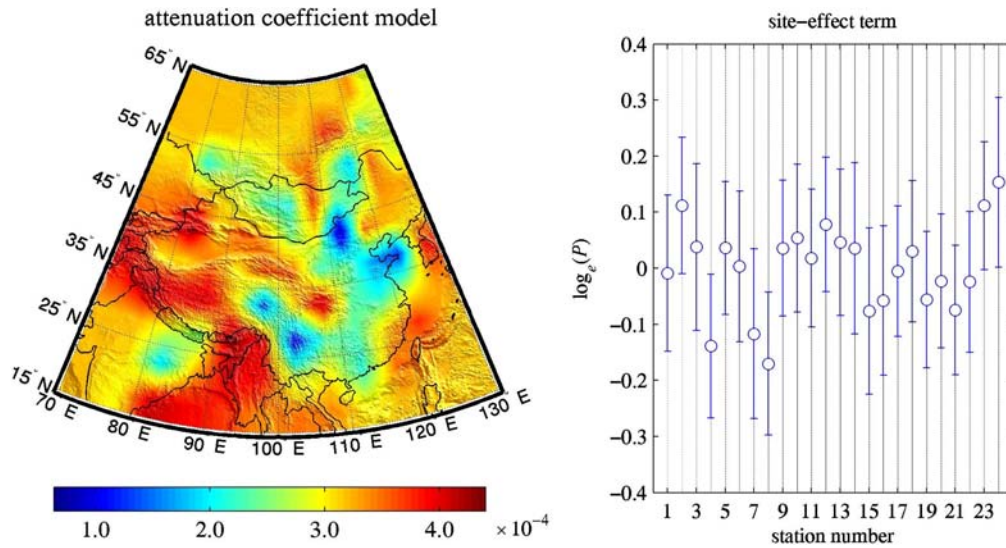


Figure 6. Estimated 20-sec Rayleigh-wave attenuation-coefficient and site-effect model from the two-station amplitude-ratio inversion. Site effects are displayed along with the error estimates. Station numbers correspond to those in Figure 5a.

ACKNOWLEDGEMENTS

We thank Anatoli Levshin and Michael Ritzwoller at University of Colorado at Boulder, and Jeffrey Stevens at Science Applications International Corporation (SAIC) for providing us with their surface-wave group-velocity models.

REFERENCES

- Brune, J. N. (1970), Tectonic stress and spectra of seismic shear waves from earthquakes, *J. Geophys. Res.*, 75, 4997-5009.
- Dziewonski, A. M., S. Bloch, and M. Landisman (1969), A technique for the analysis of transient seismic signals, *Bull. Seism. Soc. Am.*, 59, 427-444.
- Hartse, H. E., S. R. Taylor, W. S. Phillips, and G. E. Randall (1997), Regional event discrimination in central Asia with emphasis on western China, *Bull. Seism. Soc. Am.*, 87, 551-568.
- Herrin, E. T. and T. T. Goforth (1977), Phase matched filters: application to the study of Rayleigh waves, *Bull. Seism. Soc. Am.*, 67, 1259-1275.
- Herrmann, R. B. (1973), Some aspects of band-pass filtering of surface waves, *Bull. Seism. Soc. Am.*, 63, 663-671.
- Isaaks, E. H., and R. M. Srivastava (1989), *An Introduction to Applied Geostatistics*, Oxford University Press, New York, 561pp.
- Levshin, A. L., J. L. Stevens, M. H. Ritzwoller and D. A. Adams (September 2002), Short-period (7-s to 15-s) group velocity measurements and maps in central Asia, in *Proceedings of the 24th Seismic Research Review: Nuclear Explosion Monitoring: Innovation and Integration, 2002*, LA-UR-02-5048, Vol. I, 97-106.
- Mitchell, B. J., Y. Pan, J. Xie, and L. Cong (1997), Lg coda Q variation across Eurasia and its relation to crustal evolution, *J. Geophys. Res.*, 102, 22,767-22,779.
- Mitchell, B. J. (1995), Anelastic structure and evolution of the continental crust and upper mantle from seismic surface wave attenuation, *Rev. of Geophys.*, 33, 441-462.
- Phillips, W. S., H. E. Hartse, S. R. Taylor (2000), 1 Hz Lg Q tomography in central Asia, *Geophys. Res. Lett.*, 20, 3425-3428.
- Ritzwoller, M. H. and A. L. Levshin (1998), Eurasian Surface Wave Tomography: Group Velocities, *J. Geophys. Res.* 103, 4839-4878.
- Schultz, C. A., S. C. Myers, J. Hipp, and C. Young (1998), Nonstationary Bayesian Kriging: A predictive technique to generate spatial corrections for seismic detection, location, and identification, *Bull. Seism. Soc. Am.*, 88, 1275-1288.
- Stevens, J. L., D. A. Adams, and G. E. Baker (September 2001), Improved Surface Wave Detection and measurement Using Phase-Matched Filtering with a Global One-Degree Dispersion Model, in *Proceedings of the 23rd Seismic Research Review: Worldwide Monitoring of Nuclear Explosions, 2001*, LA-UR-01-4454, Vol. I, 420-430.
- Tarantola, A. (1987), *Inverse Problem Theory*, Elsevier Science, Amsterdam, The Netherlands, 630pp.
- Taylor, S. R., and H. E. Hartse (1998), A procedure for estimation of source and propagation amplitude corrections for regional seismic discriminants, *J. Geophys. Res.*, 103, 2781-2789.
- Taylor, S. R., A. A. Velasco, H. E. Hartse, W. S. Phillips, W. R. Walter, and A. J. Rodgers (2002), Amplitude corrections for regional seismic discriminants, *Pure. App. Geophys.* 159, 623-650.
- Taylor, S. R., X. Yang, and W. S. Phillips (2003), Bayesian Lg attenuation tomography applied to eastern Asia, *Bull. Seism. Soc. Am.*, 93 795-803.

25th Seismic Research Review - Nuclear Explosion Monitoring: Building the Knowledge Base

- Walter, W. R. and S. R. Taylor (2002), A revised Magnitude and Distance Amplitude Correction (MDAC2) procedure for regional seismic discriminants: Theory and testing at NTS, *Los Alamos National Laboratory*, LA-UR-02-1008, 15pp.
- Yang, X., S. R. Taylor, H. J. Patton, M. Maceira and A. A. Velasco (September 2002), Evaluation of intermediate-period (10- to 30-sec) Rayleigh-wave group-velocity maps for central Asia, in *Proceedings of the 24th Seismic Research Review: Nuclear Explosion Monitoring: Innovation and Integration, 2002*, LA-UR-02-5048, Vol. I, 609-617.